# The RNA helicases Dbp2 and Mtr4 regulate the expression of Xrn1-sensitive long non-coding RNAs in yeast

Maxime Wery, Ugo Szachnowski, Sara Andjus, Alvaro de Andres-Pablo, Antonin Morillon

Published in final edited form as:
*Front RNA Res*. ; 1: . doi:10.3389/frnar.2023.1244554.

# The RNA helicases Dbp2 and Mtr4 regulate the expression of Xrn1-sensitive long non-coding RNAs in yeast

**Maxime Wery**[1,*], **Ugo Szachnowski**[1], **Sara Andjus**[2], **Alvaro de Andres-Pablo**[1], **Antonin Morillon**[1,*]

[1]ncRNA, Epigenetic and Genome Fluidity, Institut Curie, Sorbonne Université, CNRS UMR3244, Paris Cedex, France

[2]ncRNA, Epigenetic and Genome Fluidity, Institut Curie, PSL University, Sorbonne Université, CNRS UMR3244, Paris Cedex, France

## Abstract

The expression of yeast long non-coding (lnc)RNAs is restricted by RNA surveillance machineries, including the cytoplasmic 5'-3' exonuclease Xrn1 which targets a conserved family of lncRNAs defined as XUTs, and that are mainly antisense to protein-coding genes. However, the co-factors involved in the degradation of these transcripts and the underlying molecular mechanisms remain largely unknown. Here, we show that two RNA helicases, Dbp2 and Mtr4, act as global regulators of XUTs expression. Using RNA-Seq, we found that most of them accumulate upon Dbp2 inactivation or Mtr4 depletion. Mutants of the cytoplasmic RNA helicases Ecm32, Ski2, Slh1, Dbp1, and Dhh1 did not recapitulate this global stabilization of XUTs, suggesting that XUTs decay is specifically controlled by Dbp2 and Mtr4. Notably, Dbp2 and Mtr4 affect XUTs



*Correspondence: Maxime Wery, maxime.wery@curie.fr, Antonin Morillon, antonin.morillon@curie.fr.

Edited by:
Tobias von der Haar, University of Kent, United Kingdom
Reviewed by:
Sarah Faith Newbury, University of Sussex, United Kingdom
José E. Pérez-Ortín, University of Valencia, Spain

**Author contributions**

MW and AM designed experiments. MW, SA, and AA-P performed experiments. US performed bioinformatics analyses. MW and US analyzed the data. MW and AM designed the project. MW and AM supervised the project. MW wrote the manuscript, with input from all authors. AM acquired funding. All authors contributed to the article and approved the submitted version.

**Conflict of interest**

The author MW declared that he was an editorial board member of Frontiers, at the time of submission. This had no impact on the peer review process and the final decision.
The remaining authors declare that the research was conducted in the absence of any commercial or financial relationships that could be construed as a potential conflict of interest.

**Publisher's note**

All claims expressed in this article are solely those of the authors and do not necessarily represent those of their affiliated organizations, or those of the publisher, the editors and the reviewers. Any product that may be evaluated in this article, or claim that may be made by its manufacturer, is not guaranteed or endorsed by the publisher.

**Disclaimer:** All claims expressed in this article are solely those of the authors and do not necessarily represent those of their affiliated organizations, or those of the publisher, the editors and the reviewers. Any product that may be evaluated in this article or claim that may be made by its manufacturer is not guaranteed or endorsed by the publisher.

independently of their configuration relative to their paired-sense mRNAs. Finally, we show that the effect of Dbp2 on XUTs depends on a cytoplasmic localization. Overall, our data indicate that Dbp2 and Mtr4 are global regulators of lncRNAs expression and contribute to shape the non-coding transcriptome together with RNA decay machineries.

**Keywords**

RNA helicase; Dbp2; Mtr4; Xrn1 exonuclease; lncRNA

## Introduction

The pervasive transcription of eukaryotic genomes produces plenty of long non-coding (lnc)RNAs, the identification and characterization of which have been subject to intense research for more than a decade (Jarroux et al., 2017). Besides the question of their functional significance which is still the matter of an ongoing debate (Ponting and Haerty, 2022), the molecular mechanisms controlling their biogenesis and expression remain poorly understood to date.

In organisms with compact genomes such as the budding yeast *Saccharomyces cerevisiae* (Goffeau et al., 1996), a large proportion of lncRNAs arise from the DNA strand antisense (as) to protein-coding genes. Apart from their regulatory potential (Camblong et al., 2007; Camblong et al., 2009; Van Dijk et al., 2011; Pelechano and Steinmetz, 2013; Wery et al., 2018a), one peculiarity of aslncRNAs is their low cellular abundance. In fact, previous works revealed that these transcripts are extensively degraded by the nuclear exosome and the cytoplasmic 5'-3' exoribonuclease Xrn1 (Tisseur et al., 2011). The sensitivity to these decay machineries has been used to define families of lncRNAs, including the Cryptic Unstable Transcripts (CUTs) which are targeted by the exosome (Neil et al., 2009; Xu et al., 2009), and the Xrn1-sensitive Unstable Transcripts (XUTs) which are degraded by Xrn1 (Van Dijk et al., 2011). Notably, these families of lncRNAs are conserved in other yeast species which unlike *S. cerevisiae* have maintained a functional RNA interference (RNAi) pathway, including the budding yeast *Naumovozyma castellii* (Szachnowski et al., 2019) and the distant fission yeast *Schizosaccharomyces pombe* (Atkinson et al., 2018; Wery et al., 2018b; Watts et al., 2018).

In addition to CUTs and XUTs, Nrd1-Unterminated Transcripts (NUTs) were shown to accumulate upon nuclear depletion of the RNA-binding factor Nrd1 (Schulz et al., 2013), and Stable Unannotated Transcripts (SUTs) were defined as exosome-insensitive lncRNAs that are detectable in WT cells (Xu et al., 2009), but some isoforms overlap with the XUT family distinct by their 3' extension (Wery et al., 2016).

Mechanistically, the instability of CUTs largely depends on their transcription termination by the Nrd1-Nab3-Sen1 (NNS) complex, which recruits the TRAMP4 complex (Trf4-Air2/1-Mtr4) through a direct interaction between Nrd1 and the non-canonical poly(A)-polymerase Trf4 (Tudek et al., 2014). The short poly(A) tail added by Trf4 to the target RNA then promotes the recruitment of the exosome and the degradation of the transcript (LaCava et al., 2005). In contrast, XUTs are poly-adenylated by the canonical poly(A) polymerase





Europe PMC Funders Author Manuscripts

Pap1, like mRNAs (Van Dijk et al., 2011; Wery et al., 2016). XUTs are produced as capped transcripts and therefore need to be decapped before being degraded by Xrn1 (Wery et al., 2016). Interestingly, most of them are targeted to Xrn1 by the Nonsense-Mediated mRNA Decay (NMD) pathway (Malabat et al., 2015; Wery et al., 2016), a conserved translation-dependent RNA decay pathway known to degrade aberrant mRNAs bearing a premature stop codon within the coding sequence (Losson and Lacroute, 1979; Muhlrad and Parker, 1994) as well as mRNAs with a long 3' untranslated region (Muhlrad and Parker, 1999; Amrani et al., 2004; Celik et al., 2017). On the other hand, asXUTs were shown to form double-stranded (ds)RNA structures *in vivo* with the paired-sense mRNAs, which modulates their sensitivity to NMD (Wery et al., 2016), suggesting that the dynamics of pairing with the sense mRNAs is critical for the post-transcriptional fate of the interacting aslncRNAs. In this context, we previously identified the RNA helicases Dbp2 and Mtr4 as potential actors involved in the degradation of asXUTs, possibly by promoting dsRNA unwinding (Wery et al., 2016). Dbp2 belongs to the DEAD-box RNA helicase family and is highly conserved among eukaryotes (Xing et al., 2019). Its human ortholog (DDX5) has been functionally associated to cancers (Secchi et al., 2022). Dbp2/DDX5 impacts RNA metabolism by different way, including RNA decay and NMD. In fact, Dbp2 was reported to physically interact with the NMD core factor Upf1 (Bond et al., 2001). Although Dbp2 is predominantly nuclear, it can localize in the cytoplasm under particular conditions (Beck et al., 2014). Mtr4 is a nuclear DExH-box RNA helicase endowed with an ATP-dependent 3'–5' helicase activity which could unwind dsRNA with a 3' extension (Bernstein et al., 2008), as proposed for XUTs (Wery et al., 2016).

This idea that Dbp2 and Mtr4 could contribute to regulate the expression of XUTs was based on the observation that two of them, namely, *XUT0741* and *XUT1678* (antisense to the *ADH2* and *ARG1* mRNAs, respectively), accumulate in *dbp2Δ* cells or upon depletion of Mtr4 (Wery et al., 2016). However, the effect of these helicases on the entire XUTs family remained unexplored.

Here, we report that Dbp2 and Mtr4 are global regulators of XUTs expression. Using RNA-Seq, we show that most XUTs accumulate upon Dbp2 loss or Mtr4 depletion. This effect is not a common feature of RNA helicase mutants since XUTs levels remained unchanged in cells lacking the Ecm32, Ski2, Slh1, Dbp1 or Dhh1 helicases. Notably, the effect of Dbp2 and Mtr4 is independent of the configuration of XUTs relative to their sense-paired mRNAs. Finally, we show that nuclear depletion of Dbp2 does not affect XUTs expression, indicating that the effect of Dbp2 on XUTs depends on a cytoplasmic localization.

Altogether, our data indicate that Dbp2 and Mtr4 are important factors that globally contribute to the control of lncRNAs expression and the shaping of the non-coding transcriptome.

## Materials and methods

### Yeast strains and media

All the experiments have been performed using strains of the closely related S288C and W303/BMA64-1A genetic backgrounds (Supplementary Table S2). Cells were grown

to mid-log phase in YPD medium at 30°C. For Mtr4-depletion, WT (YAM115) and *tetOFF::MTR4(YAM997)* cells were grown to mid-log phase in YPD at 30°C, before addition of doxycycline at 10 μg/mL (final concentration) for 6 h. During this treatment, cells were maintained to mid-log phase ($OD_{600}$ 0.5) by dilution into preheated YPD medium with 10 μg/mL doxycyline. For the Dbp2 anchor-away experiment, parental (YAM2672) and Dbp2-FRB-GFP (YAM2673) cells were grown to mid-log phase in YPD at 30°C, before addition of rapamycin at 1 μg/mL (final concentration) for 1 h.

### Total RNA extraction

Total RNA was extracted from cells grown to mid-log phase ($OD_{600}$ 0.5) using standard hot phenol procedure. Extracted RNA was ethanol-precipitated, resuspended in nuclease-free $H_2O$ (Ambion) and quantified using a NanoDrop 2000c spectrophotometer and/or a Qubit fluorometer with the Qubit RNA HS Assay kit (Life Technologies).

### Strand-specific RT-qPCR

Strand-specific RT-qPCR experiments were performed from three biological replicates, using 1 μg of total RNA and the SuperScript II Reverse Transcriptase (Invitrogen) in the presence of 6.25 μg/mL actinomycin D, as previously described (Wery et al., 2018a). The oligonucleotides used are listed in Supplementary Table S3.

### Total RNA-Seq

For each strain/condition, total RNA-Seq was performed from two biological replicates. For each sample, 1 μg of total RNA was mixed with 2 μL of diluted ERCC RNA spike-in mix (1:100 dilution in nuclease-free $H_2O$; Invitrogen). Ribosomal (r)RNAs were depleted using the RiboMinus Eukaryote v2 kit (Ambion), and rRNA-depleted RNAs were then concentrated using the RiboMinus Concentration Module (Invitrogen).

For *dbp2Δ, dbp2-AA* and *tetOFF::MTR4* (and their respective WT control), strand-specific RNA-seq libraries were prepared from 125 ng of rRNA-depleted RNAs using the TruSeq Stranded Total RNA kit (Illumina). Libraries concentration was determined using the Qubit DNA HS Assay kit (Life Technologies), and their quality was controlled upon analysis on a High Sensitivity DNA Assay chip in a 2100 bioanalyzer (Agilent). Paired-end sequencing (50 nt + 50 nt) of the libraries was performed on a HiSeq 2500 sequencer (Illumina).

Libraries preparation for the *ecm32Δ, slh1Δ, ski2Δ, dbp1Δ* and *dhh1Δ* mutants (and the isogenic WT control) was similar, except that they were constructed from 50 ng of rRNA-depleted RNAs using the TruSeq Stranded mRNA kit (Illumina). Paired-end sequencing (50 nt + 50 nt) was performed on a NovaSeq 6000 system (Illumina).

### Total RNA-Seq data processing and analysis

Briefly, reads were trimmed using Trim Galore (https://github.com/FelixKrueger/TrimGalore). They were then mapped on the S288C reference genome (R64-2-1, including the 2-micron plasmid), with addition of ERCC RNA spike-in sequences (Ambion) using version 2.2.0 of Hisat (Kim et al., 2019), with default parameters and a maximum size for introns of 5000 nt. Uniquely mapped reads were used for all subsequent analyses.

Gene counts were determined using featureCounts v2.0.0 (Liao et al., 2014), and then normalized using the estimate Size factorsForMatrix function of DESeq2 (Love et al., 2014). Tag densities were obtained as: normalized gene count/gene length.

Given the effect of Dbp2 inactivation and Mtr4 depletion on snoRNAs (Supplementary Figures S1A, S1B), the corresponding RNA-Seq data were normalized on the ERCC RNA spike-in signal. In contrast, since inactivation of Ecm32, Slh1, Ski2, Dbp1 and Dhh1 had no effect on them, snoRNAs levels were used for normalization of RNA-Seq signals, as previously described (Wery et al., 2016; Wery et al., 2018b; Andjus et al., 2022). Normalization factors can be found in Supplementary Table S4.

Significantly up-regulated XUTs were determined as previously described (Andjus et al., 2022), using i) a minimal fold-change of 2 in the condition of interest *vs*. the corresponding WT/control and ii) an adjusted *p*-value ≤ 0.05 upon differential expression analysis using DESeq2 (Love et al., 2014).

## Results

### Most XUTs accumulate upon inactivation of Dbp2 and Mtr4

In a previous analysis, we found that two XUTs accumulate upon inactivation of Dbp2 or depletion of Mtr4 (Wery et al., 2016). In order to extend these observations at the genome-wide level, we performed RNA-seq analysis using biological duplicates of a *dbp2Δ* strain deleted for *DBP2* and the isogenic WT control. In the case of Mtr4 (which is an essential gene), we used a conditional *tetOFF::MTR4* mutant, where *MTR4* is under the control of a *tetOFF* promoter, repressed in the presence of doxycycline (dox). Both the conditional mutant and its isogenic WT were treated with dox for 6 h, which is the time necessary to deplete the helicase but keeping the cells alive and growing (Wery et al., 2016).

Dbp2 and Mtr4 participate in transcriptome regulation and their inactivation alters several families of transcripts (Beck et al., 2014). For instance, snoRNAs which we classically used to normalize *xrn1Δ* RNA-seq data because they are insensitive to Xrn1 (Wery et al., 2016), are deregulated upon Mtr4 inactivation (van Hoof et al., 2000). For this reason, we decided to add a spike-in to the total RNA used to prepare the libraries and use it to normalize the RNA-seq signals.

Our RNA-seq data show that XUTs are globally sensitive to Dbp2 and Mtr4 (Figure 1A; see also Supplementary Figures S1A, S1B). Strikingly, the mean fold enrichment of XUTs was higher in Mtr4-depleted cells than in the *dbp2Δ* mutant (Figures 1B, C; see also Supplementary Figures S1C, S1D). In contrast, the stabilization of protein-coding transcripts was very similar between the two conditions (Figures 1B, C; see also Supplementary Figure S1C). We also noted that the global sensitivity of XUTs to Dbp2 is significantly lower than their sensitivity to NMD (Upf1) and Xrn1 (Supplementary Figure S1D). Strikingly, CUTs and NUTs display the highest sensitivity to Mtr4 (Figure 1C; Supplementary Figure S1C), which is consistent with the role of this helicase in their decay (Bernstein et al., 2010). As discussed below, the fact that many XUTs overlap CUTs and/or NUTs probably explains (at least partially) the high sensitivity of XUTs to Mtr4 (Supplementary Figure S1D).

The number of Dbp2-and Mtr4-sensitive XUTs was determined using a minimal fold-change of 2 and a *p*-value < 0.05 upon differential expression analysis using DESeq2 (Love et al., 2014), showing that 1077 (64.7%) and 1547 (92.9%) XUTs are sensitive to Dbp2 and Mtr4, respectively (Figures 1D, E; see also Supplementary Table S1). A comparison between the targets of each helicase revealed that 1040 XUTs (62.5% of the total) are sensitive to both helicases; 507 and 37 XUTs are Mtr4- and Dbp2-specific, respectively (Figures 1D, E; see also Supplementary Table S1). Statistical analysis shows that the number of XUTs targeted by both Dbp2 and Mtr4 is significantly higher than expected by chance ($p < 0.001$, Chi-square test of independence), indicating that when a XUT is targeted by one helicase, it is also more prone to be targeted by the second.

In order to validate the results obtained by RNA-seq, four XUTs were selected for quantification using strand-specific RT-qPCR. According to the RNA-seq data, three of these XUTs *(XUT1051, XUT0745* and *XUT0420)* are sensitive to both helicases, while the last *(XUT0007)* is specific to Mtr4 (see Supplementary Table S1). The results obtained by RT-qPCR correlate with the RNA-Seq, thereby validating the observations made at the genome-wide level (see Supplementary Figures S1E, S1F).

Together, these results indicate that Dbp2 and Mtr4 globally control the expression of XUTs, many of them being targeted by both helicases, suggesting a possible redundancy between them.

## XUTs are globally insensitive to the cytoplasmic helicases Ecm32, Ski2, Slh1, Dbp1 and Dhh1

The RNA-Seq analysis described above revealed the role of Dbp2 and Mtr4 in the control of XUTs expression. We asked whether other helicases could also be implicated. Since XUTs are degraded in the cytoplasm and given the role of NMD and translation in their metabolism (Wery et al., 2016; Andjus et al., 2022), we decided to focus on five cytoplasmic RNA helicases, including Ecm32, Ski2, Slh1, Dbp1 and Dhh1, involved in translation regulation and/or mRNA decay.

Ecm32 (also known as Mtt1) is an Upf1-like helicase associated to polysomes and shown to interact with the translation termination factor eRF3 (Czaplinski et al., 2000). Ski2 is a component of the Ski complex, mediating 3'-5' mRNA degradation by the cytoplasmic form of the exosome (Anderson and Parker, 1998). Slh1 is a Ski2-like helicase and is part of the ribosome-associated quality control trigger (RQT) complex (Sitron et al., 2017). Dbp1 is a DEAD-box RNA helicase promoting translation initiation (Sen et al., 2019). Dhh1 belongs to the same family of DEAD box helicases and stimulates mRNA decapping (Coller et al., 2001).

To assess the potential effect of these helicases on XUTs expression, we performed RNA-Seq in *ecm32Δ, ski2Δ, slh1Δ, dbp1Δ* and *dhh1Δ* mutant cells (Figures 2A, B). In sharp contrast to Dbp2 and Mtr4, we identified no differentially expressed XUT in the *ecm32Δ* and *s1h1Δ*mutants (Supplementary Figures S2A, S2B). Globally, XUTs levels even slightly decreased in absence of Slh1 (Figure 2B; $p = 1.20^{e-03}$, two-sided Wilcoxon rank-sum test). Inactivation of Ski2, Dbp1 and Dhh1 led to a significant accumulation of 2, 8 and 7

XUTs, respectively (Supplementary Figure S2C–S2E; see also Supplementary Table S1), but these effects remain marginal in comparison to the impact of Dbp2 inactivation and Mtr4 depletion (Figures 2A, B). Interestingly, 185 XUTs were significantly down-regulated in *dhh1Δ* cells (Supplementary Figure S2E; see also Supplementary Table S1), suggesting that Dhh1 does not act by promoting the degradation of XUTs but rather contributes to stabilize them. Consistent with this idea, the global levels of XUTs significantly decrease in Dhh1-lacking cells (Figure 2B; $p = 2.83^{e-51}$, two-sided Wilcoxon rank-sum test).

In conclusion, the effect of the cytoplasmic RNA helicases Ecm32, Slh1, Ski2, Dbp1 and Dhh1 on XUTs decay is marginal in comparison to Dbp2 and Mtr4. Our data suggest that Dhh1 could even have an opposite effect, contributing to protect XUTs from decay.

## The Mtr4-sensitivity of a subset of XUTs probably reflects an effect on the overlapping CUTs/NUTs

Mtr4 depletion results in a strong accumulation of CUTs and NUTs (Figure 1C). These transcripts are degraded by the nuclear exosome, assisted by the TRAMP4 complex which contains Mtr4 (LaCava et al., 2005). This probably explains the accumulation of CUTs and NUTs upon Mtr4 depletion. Given the overlap between some XUTs and CUTs/NUTs (Wery et al., 2016), the global accumulation of XUTs could actually reflect an effect on the overlapping CUTs/NUTs. To overcome this problem, we separated XUTs into two subsets, based on the absence ($XUT^a$) or existence ($XUT^b$) of overlap (>1 nt) with a CUT or NUT. As one could expect, the two subsets of XUTs display different sensitivity to Mtr4, the $XUT^b$ subset showing a stronger stabilization upon Mtr4 depletion (close to that of CUTs/NUTs), whereas $XUT^a$showed a moderate stabilization (Supplementary Figures S3A, S3B).

The subsequent analyses were therefore performed using the $XUT^a$ subset only.

## Dbp2 and Mtr4 target XUTs independently of their configuration to protein-coding genes

In a previous report, we proposed that asXUTs displaying a single-stranded (ss) 3’ extension would be preferentially targeted by NMD (Wery et al., 2016). This prompted us to investigate the configuration of Dbp2-sensitive and Mtr4-sensitive XUTs.

XUTs were separated in five types according to the possibility of their 5’- and 3’-ends to engage in a dsRNA structure with the paired-sense mRNA (Figure 3A). The observed number of Dbp2-sensitive XUTs displaying a free 3’-end (types 4 and 5) was slightly higher than expected, whereas the number of those fully engaged in dsRNA with the paired-end sense mRNA (type 2) was slightly lower (Figure 3B). Surprisingly, the number of “solo” Dbp2-sensitive XUTs (type 1) was higher than expected by chance. However, these differences were not significant ($p = 0.073$, Chi-square test of independence), thereby indicating that Dbp2 does not preferentially target one type of XUTs.

We performed a similar analysis using the Mtr4-sensitive XUTs among the $XUT^a$ subset and reached the same conclusion (Figure 3C, $p = 0.913$, Chi-square test of independence). Further indicating that Dbp2 and Mtr4 target XUTs independently of their configuration relative to sense mRNA, the mean and median fold-change was similar for the different types of XUTs (Supplementary Figures S3C, S3D).

These observations therefore lead us to conclude that Dbp2 and Mtr4 regulate XUTs expression, regardless their configuration relative to the paired-sense mRNAs.

### Dbp2 acts on XUTs in the cytoplasm

Dbp2 has a predominant nuclear localization, and it has been proposed to repress cryptic antisense transcription (Cloutier et al., 2012). However, it can also localize in the cytoplasm under some conditions. Furthermore, it can physically interact with the NMD core factor Upf1 (Bond et al., 2001), which is localized in the cytoplasm.

The data described above show that Dbp2 inactivation results in a global accumulation of XUTs. However, whether Dbp2 acts on XUTs in the nucleus (possibly at the transcriptional level) or in the cytoplasm remains unclear.

In order to address this question, we decided to use the anchor-away technique (Haruki et al., 2008), which enables to deplete from the nucleus a protein fused to a FKBP12 rapamycin-binding (FRB) domain upon treatment with rapamycin (Figure 4A). We used a published Dbp2-FRB-GFP strain and depleted Dbp2 from the nucleus using a 60 min treatment with rapamycin, as previously described (Cloutier et al., 2016).

The nuclear depletion of the protein was validated by fluorescence microscopy on living cells. Before rapamycin treatment, the Dbp2-FRB-GFP protein appeared as a clear single spot within the cell, but 60 min after rapamycin addition, the protein showed a diffuse signal within the cells (Supplementary Figure S4A), consistent with previously published observations (Cloutier et al., 2016).

In a first time, we tested the effect of the nuclear depletion of Dbp2 on three Dbp2-sensitive XUTs using RT-qPCR. This analysis was performed in Dbp2-FRB-GFP *(dbp2-AA)* cells and the isogenic parental strain, with or without rapamycin treatment, so that we could also assess the effect of FRB- and GFP-tagging on the activity of Dbp2. Notably, none of the three tested XUTs significantly accumulated following nuclear depletion of Dbp2, their levels being similar before and after the treatment with rapamycin (Figure 4B). However, we noted that the levels of the three XUTs significantly increased in the Dbp2-FRB-GFP strain in absence of rapamycin treatment, compared to the parental strain in the same condition (Supplementary Figure S4B). This indicates that Dbp2 tagging partially impacts the activity of Dbp2.

These observations were then extended at the genome-wide level using RNA-Seq, showing that XUTs levels remain unchanged upon nuclear depletion of Dbp2 (Figures 4C, D; see also Supplementary Table S1; Supplementary Figures S4C, S4D).

From these experiments, we conclude that nuclear depletion of Dbp2 does not affect XUTs expression, which is consistent with the idea that Dbp2 targets them in the cytoplasm.

## Discussion

In yeast, lncRNAs expression is restricted by RNA decay machineries, including the 5’-3’ exoribonuclease Xrn1 which degrades a conserved class of cytoplasmic lncRNAs defined

as XUTs, predominantly antisense to protein-coding genes. Interestingly, the stabilization of XUTs correlates with the transcriptional attenuation of a subset of genes in *S. cerevisiae* (Van Dijk et al., 2011) and also in *S. pombe* (Wery et al., 2018a), suggesting that XUTs could be involved in the regulation of gene expression.

Besides their regulatory potential, previous studies revealed that a large fraction of XUTs are targeted to Xrn1 by the NMD pathway, and that this sensitivity to NMD can be modulated by the formation of dsRNA structures (Wery et al., 2016). In this context, here we show that two RNA helicases act as additional regulators of XUTs expression. RNA-Seq analyses revealed that most XUTs accumulate in cells lacking Dbp2 or depleted for Mtr4. The majority of them are targeted by both Dbp2 and Mtr4, suggesting a redundancy between the two helicases. Whether the two helicases compete for the same XUTs or cooperate to ensure that they are properly targeted to the decay remains unknown. However, we noted that the mean fold-enrichment for XUTs was significantly higher in Mtr4-depleted than in *dbp2Δ* cells, even after filtering out those XUTs overlapping highly Mtr4-sensitive CUTs and NUTs ($XUT^a$ subset). This indicates that XUTs might be preferentially targeted by Mtr4.

In terms of subcellular localization, Mtr4 is nuclear (LaCava et al., 2005), suggesting that it acts on XUTs before their export to the cytoplasm. On the other hand, even if Dbp2 is predominantly nuclear, it can be redistributed into the cytoplasm (Beck et al., 2014). Dbp2 has also been reported to physically interact with the NMD core factor Upf1, which are localized in the cytoplasm (Sheth and Parker, 2006). Taken together, these observations lead us to propose a model where Mtr4 would be the first helicase acting on XUTs in the nucleus. Dbp2 would act in a second time, after export of XUTs to the cytoplasm. This scenario is supported by the observation that nuclear depletion of Dbp2 does not result into XUTs accumulation, indicating that the effect of Dbp2 on XUTs does not involve a nuclear localization.

Further experiments are required to decipher the molecular mechanism by which the two RNA helicases act on XUTs and understand the biological importance of their action for the cell. Dbp2 has been proposed to repress cryptic transcription (Cloutier et al., 2012). According to this model, the inactivation of Dbp2 could increase XUTs expression at the transcriptional level. Our RNA-Seq approach does not allow to determine whether the higher abundance of XUTs in *dbp2Δ* cells reflects a transcriptional and/or post-transcriptional effect. However, the anchor-away experiment showed that delocalizing Dbp2 out of the nucleus does not result into accumulation of XUTs, which is not in favor of a model where Dbp2 would act at the level of transcription by repressing XUTs expression. Native Elongating Transcript sequencing (NET-Seq) experiments in *dbp2Δ* cells could be considered to specifically address this question (Wery et al., 2018b).

Finally, it remains to be tested whether the effect of Dbp2 and Mtr4 on XUTs depends on their respective helicase activity. In fact, the observations that both helicases target XUTs independently of their configuration to the paired-sense mRNAs, and in particular “solo” XUTs, raise the question of the requirement of the helicase activity. Construction and functional characterization of mutant strains carrying point mutations in the ATP-dependent helicase domain of Dbp2 and Mtr4 would help to address this.

Overall, by identifying two additional regulators of Xrn1-sensitive lncRNAs expression, our work provides insight into the pathway by which the cell regulates and shapes the non-coding transcriptome. The high degree of conservation of the actors identified in yeast opens exciting perspectives regarding their potential contribution in regulating the expression of lncRNAs in other eukaryotic models, including human cells.

## Supplementary Material

Refer to Web version on PubMed Central for supplementary material.

## Acknowledgements

We would like to thank Sara Cloutier and Elizabeth Tran for the *dbp2Δ* and *dbp2-AA* strains, as well as Alice Lebreton and Bertrand Séraphin for sharing with us their unpublished *tetOFF::MTR4* (BSY1756) strain. We are also grateful to Camille Gautier for preliminary bioinformatics analyses. Data management, quality control and primary analysis were performed by the Bioinformatics platform of the Institut Curie.

### Funding

This work has benefited from the ANR “DNA-life” (ANR-15-CE12-0007) grant and the ERC “DARK” consolidator grant allocated to AM. High-throughput sequencing was performed by the ICGex NGS platform of the Institut Curie supported by the grants ANR-10-EQPX-03 (Equipex) and ANR-10-INBS-09-08 (France Génomique Consortium) from the Agence Nationale de la Recherche (“Investissements d’Avenir” program), by the ITMO-Cancer Aviesan (Plan Cancer III) and by the SiRIC-Curie program (SiRIC Grant INCa-DGOS-465 and INCa-DGOSInserm_12554). SA has been supported by a PhD fellowship from PSL University and by the Fondation pour la Recherche Médicale (FRM).

## Data availability statement

Raw sequences generated in this work have been deposited to the NCBI Gene Expression Omnibus and can be accessed using accession number GSE235554. Genome browsers for visualization of processed data are publicly accessible at http://vm-gb.curie.fr/dbp2_mtr4/.

## References

Amrani N, Ganesan R, Kervestin S, Mangus DA, Ghosh S, Jacobson A. A faux 3’-UTR promotes aberrant termination and triggers nonsense-mediated mRNA decay. Nature. 2004; 432 (7013) 112–118. DOI: 10.1038/nature03060 [PubMed: 15525991]

Anderson JS, Parker RP. The 3’ to 5’ degradation of yeast mRNAs is a general mechanism for mRNA turnover that requires the SKI2 DEVH box protein and 3’ to 5’ exonucleases of the exosome complex. EMBO J. 1998; 17 (5) 1497–1506. DOI: 10.1093/emboj/17.5.1497 [PubMed: 9482746]

Andjus S, Szachnowski U, Vogt N, Hatin I, Papadopoulos C, Lopes A, et al. Translation is a key determinant controlling the fate of cytoplasmic long non-coding RNAs. bioRxiv. 2022; doi: 10.1101/2022.05.25.493276

Atkinson SR, Marguerat S, Bitton DA, Rodriguez-Lopez M, Rallis C, Lemay JF, et al. Long noncoding RNA repertoire and targeting by nuclear exosome, cytoplasmic exonuclease, and RNAi in fission yeast. RNA. 2018; 24 (9) 1195–1213. DOI: 10.1261/rna.065524.118 [PubMed: 29914874]

Beck ZT, Cloutier SC, Schipma MJ, Petell CJ, Kit W, Tran EJ. Regulation of glucose-dependent gene expression by the RNA helicase Dbp2 in*Saccharomyces cerevisiae*. Genetics. 2014; 198 (3) 1001–1014. DOI: 10.1534/genetics.114.170019 [PubMed: 25164881]

Bernstein J, Ballin JD, Patterson DN, Wilson GM, Toth EA. Unique properties of the Mtr4p-poly(A) complex suggest a role in substrate targeting. Biochemistry. 2010; 49 (49) 10357–10370. DOI: 10.1021/bi101518x [PubMed: 21058657]

Bernstein J, Patterson DN, Wilson GM, Toth EA. Characterization of the essential activities of*Saccharomyces cerevisiae*Mtr4p, a 3'->5' helicase partner of the nuclear exosome. J Biol Chem. 2008; 283 (8) 4930–4942. DOI: 10.1074/jbc.m706677200 [PubMed: 18096702]

Bond AT, Mangus DA, He F, Jacobson A. Absence of Dbp2p alters both nonsense-mediated mRNA decay and rRNA processing. Mol Cell Biol. 2001; 21 (21) 7366–7379. DOI: 10.1128/mcb.21.21.7366-7379.2001 [PubMed: 11585918]

Camblong J, Beyrouthy N, Guffanti E, Schlaepfer G, Steinmetz LM, Stutz F. Trans-acting antisense RNAs mediate transcriptional gene cosuppression in*S. cerevisiae*. Genes Dev. 2009; 23 (13) 1534–1545. DOI: 10.1101/gad.522509 [PubMed: 19571181]

Camblong J, Iglesias N, Fickentscher C, Dieppois G, Stutz F. Antisense RNA stabilization induces transcriptional gene silencing via histone deacetylation in*S. cerevisiae*. Cell. 2007; 131 (4) 706–717. DOI: 10.1016/j.cell.2007.09.014 [PubMed: 18022365]

Celik A, Baker R, He F, Jacobson A. High-resolution profiling of NMD targets in yeast reveals translational fidelity as a basis for substrate selection. RNA. 2017; 23 (5) 735–748. DOI: 10.1261/rna.060541.116 [PubMed: 28209632]

Cloutier SC, Ma WK, Nguyen LT, Tran EJ. The DEAD-box RNA helicase Dbp2 connects RNA quality control with repression of aberrant transcription. J Biol Chem. 2012; 287 (31) 26155–26166. DOI: 10.1074/jbc.m112.383075 [PubMed: 22679025]

Cloutier SC, Wang S, Ma WK, Al Husini N, Dhoondia Z, Ansari A, et al. Regulated Formation of lncRNA-DNA hybrids enables faster transcriptional induction and environmental adaptation. Mol Cell. 2016; 61 (3) 393–404. DOI: 10.1016/j.molcel.2015.12.024 [PubMed: 26833086]

Coller JM, Tucker M, Sheth U, Valencia-Sanchez MA, Parker R. The DEAD box helicase, Dhh1p, functions in mRNA decapping and interacts with both the decapping and deadenylase complexes. RNA. 2001; 7 (12) 1717–1727. DOI: 10.1017/s135583820101994x [PubMed: 11780629]

Czaplinski K, Majlesi N, Banerjee T, Peltz SW. Mtt1 is a Upf1-like helicase that interacts with the translation termination factors and whose overexpression can modulate termination efficiency. RNA. 2000; 6 (5) 730–743. DOI: 10.1017/s1355838200992392 [PubMed: 10836794]

Goffeau A, Barrell BG, Bussey H, Davis RW, Dujon B, Feldmann H, et al. Life with 6000 genes. Science. 1996; 274: 546–567. DOI: 10.1126/science.274.5287.546 [PubMed: 8849441]

Haruki H, Nishikawa J, Laemmli UK. The anchor-away technique: Rapid, conditional establishment of yeast mutant phenotypes. Mol Cell. 2008; 31 (6) 925–932. DOI: 10.1016/j.molcel.2008.07.020 [PubMed: 18922474]

Jarroux J, Morillon A, Pinskaya M. History, discovery, and classification of lncRNAs. Adv Exp Med Biol. 2017; 1008: 1–46. DOI: 10.1007/978-981-10-5203-3_1 [PubMed: 28815535]

Kim D, Paggi JM, Park C, Bennett C, Salzberg SL. Graph-based genome alignment and genotyping with HISAT2 and HISAT-genotype. Nat Biotechnol. 2019; 37 (8) 907–915. DOI: 10.1038/s41587-019-0201-4 [PubMed: 31375807]

LaCava J, Houseley J, Saveanu C, Petfalski E, Thompson E, Jacquier A, et al. RNA degradation by the exosome is promoted by a nuclear polyadenylation complex. Cell. 2005; 121 (5) 713–724. DOI: 10.1016/j.cell.2005.04.029 [PubMed: 15935758]

Liao Y, Smyth GK, Shi W. featureCounts: an efficient general purpose program for assigning sequence reads to genomic features. Bioinformatics. 2014; 30 (7) 923–930. DOI: 10.1093/bioinformatics/btt656 [PubMed: 24227677]

Losson R, Lacroute F. Interference of nonsense mutations with eukaryotic messenger RNA stability. Proc Natl Acad Sci U S A. 1979; 76 (10) 5134–5137. DOI: 10.1073/pnas.76.10.5134 [PubMed: 388431]

Love MI, Huber W, Anders S. Moderated estimation of fold change and dispersion for RNA-seq data with DESeq2. Genome Biol. 2014; 15 (12) 550. doi: 10.1186/s13059-014-0550-8 [PubMed: 25516281]

Malabat C, Feuerbach F, Ma L, Saveanu C, Jacquier A. Quality control of transcription start site selection by nonsense-mediated-mRNA decay. Elife. 2015; 4 e06722 doi: 10.7554/elife.06722 [PubMed: 25905671]

Muhlrad D, Parker R. Aberrant mRNAs with extended 3' UTRs are substrates for rapid degradation by mRNA surveillance. RNA. 1999; 5 (10) 1299–1307. DOI: 10.1017/s1355838299990829 [PubMed: 10573121]

Muhlrad D, Parker R. Premature translational termination triggers mRNA decapping. Nature. 1994; 370 (6490) 578–581. DOI: 10.1038/370578a0 [PubMed: 8052314]

Neil H, Malabat C, d'Aubenton-Carafa Y, Xu Z, Steinmetz LM, Jacquier A. Widespread bidirectional promoters are the major source of cryptic transcripts in yeast. Nature. 2009; 457 (7232) 1038–1042. DOI: 10.1038/nature07747 [PubMed: 19169244]

Pelechano V, Steinmetz LM. Gene regulation by antisense transcription. Nat Rev Genet. 2013; 14 (12) 880–893. DOI: 10.1038/nrg3594 [PubMed: 24217315]

Ponting CP, Haerty W. Genome-wide analysis of human long noncoding RNAs: A provocative review. Annu Rev Genomics Hum Genet. 2022; 23: 153–172. DOI: 10.1146/annurev-genom-112921-123710 [PubMed: 35395170]

Schulz D, Schwalb B, Kiesel A, Baejen C, Torkler P, Gagneur J, et al. Transcriptome surveillance by selective termination of noncoding RNA synthesis. Cell. 2013; 155 (5) 1075–1087. DOI: 10.1016/j.cell.2013.10.024 [PubMed: 24210918]

Secchi M, Lodola C, Garbelli A, Bione S, Maga G. DEAD-box RNA helicases DDX3X and DDX5 as oncogenes or oncosuppressors: A network perspective. Cancers (Basel). 2022; 14 (15) 3820. doi: 10.3390/cancers14153820 [PubMed: 35954483]

Sen ND, Gupta N, KArcher S, Preiss T, Lorsch JR, Hinnebusch AG. Functional interplay between DEAD-box RNA helicases Ded1 and Dbp1 in preinitiation complex attachment and scanning on structured mRNAs*in vivo*. Nucleic Acids Res. 2019; 47 (16) 8785–8806. DOI: 10.1093/nar/gkz595 [PubMed: 31299079]

Sheth U, Parker R. Targeting of aberrant mRNAs to cytoplasmic processing bodies. Cell. 2006; 125 (6) 1095–1109. DOI: 10.1016/j.cell.2006.04.037 [PubMed: 16777600]

Sitron CS, Park JH, Brandman O. Asc1, Hel2, and Slh1 couple translation arrest to nascent chain degradation. RNA. 2017; 23 (5) 798–810. DOI: 10.1261/rna.060897.117 [PubMed: 28223409]

Szachnowski U, Andjus S, Foretek D, Morillon A, Wery M. Endogenous RNAi pathway evolutionarily shapes the destiny of the antisense lncRNAs transcriptome. Life Sci Alliance. 2019; 2 (5) e201900407 doi: 10.26508/lsa.201900407 [PubMed: 31462400]

Tisseur M, Kwapisz M, Morillon A. Pervasive transcription-lessons from yeast. Biochimie. 2011; 93 (11) 1889–1896. DOI: 10.1016/j.biochi.2011.07.001 [PubMed: 21771634]

Tudek A, Porrua O, Kabzinski T, Lidschreiber M, Kubicek K, Fortova A, et al. Molecular basis for coordinating transcription termination with noncoding RNA degradation. Mol Cell. 2014; 55 (3) 467–481. DOI: 10.1016/j.molcel.2014.05.031 [PubMed: 25066235]

Van Dijk EL, Chen CL, d'Aubenton-Carafa Y, Gourvennec S, Kwapisz M, Roche V, et al. XUTs are a class of Xrn1-sensitive antisense regulatory non coding RNA in yeast. Nature. 2011; 475 (7354) 114–117. DOI: 10.1038/nature10118 [PubMed: 21697827]

van Hoof A, Lennertz P, Parker R. Yeast exosome mutants accumulate 3'-extended polyadenylated forms of U4 small nuclear RNA and small nucleolar RNAs. Mol Cell Biol. 2000; 20 (2) 441–452. DOI: 10.1128/mcb.20.2.441-452.2000 [PubMed: 10611222]

Watts BR, Wittmann S, Wery M, Gautier C, Kus K, Birot A, et al. Histone deacetylation promotes transcriptional silencing at facultative heterochromatin. Nucleic Acids Res. 2018; 46 (11) 5426–5440. DOI: 10.1093/nar/gky232 [PubMed: 29618061]

Wery M, Descrimes M, Vogt N, Dallongeville AS, Gautheret D, Morillon A. Nonsense-Mediated decay restricts LncRNA levels in yeast unless blocked by double-stranded RNA structure. Mol Cell. 2016; 61 (3) 379–392. DOI: 10.1016/j.molcel.2015.12.020 [PubMed: 26805575]

Wery M, Gautier C, Descrimes M, Yoda M, Migeot V, Hermand D, et al. Bases of antisense lncRNA-associated regulation of gene expression in fission yeast. PLoS Genet. 2018a; 14 (7) e1007465 doi: 10.1371/journal.pgen.1007465 [PubMed: 29975684]

Wery M, Gautier C, Descrimes M, Yoda M, Vennin-Rendos H, Migeot V, et al. Native elongating transcript sequencing reveals global anti-correlation between sense and antisense nascent transcription in fission yeast. RNA. 2018b; 24 (2) 196–208. DOI: 10.1261/rna.063446.117 [PubMed: 29114019]

Xing Z, Ma WK, Tran EJ. The DDX5/Dbp2 subfamily of DEAD-box RNA helicases. Wiley Interdiscip Rev RNA. 2019; 10 (2) e1519 doi: 10.1002/wrna.1519 [PubMed: 30506978]

Xu Z, Wei W, Gagneur J, Perocchi F, Clauder-Munster S, Camblong J, et al. Bidirectional promoters generate pervasive transcription in yeast. Nature. 2009; 457 (7232) 1033–1037. DOI: 10.1038/nature07728 [PubMed: 19169243]



Europe PMC Funders Author Manuscripts

Europe PMC Funders Author Manuscripts

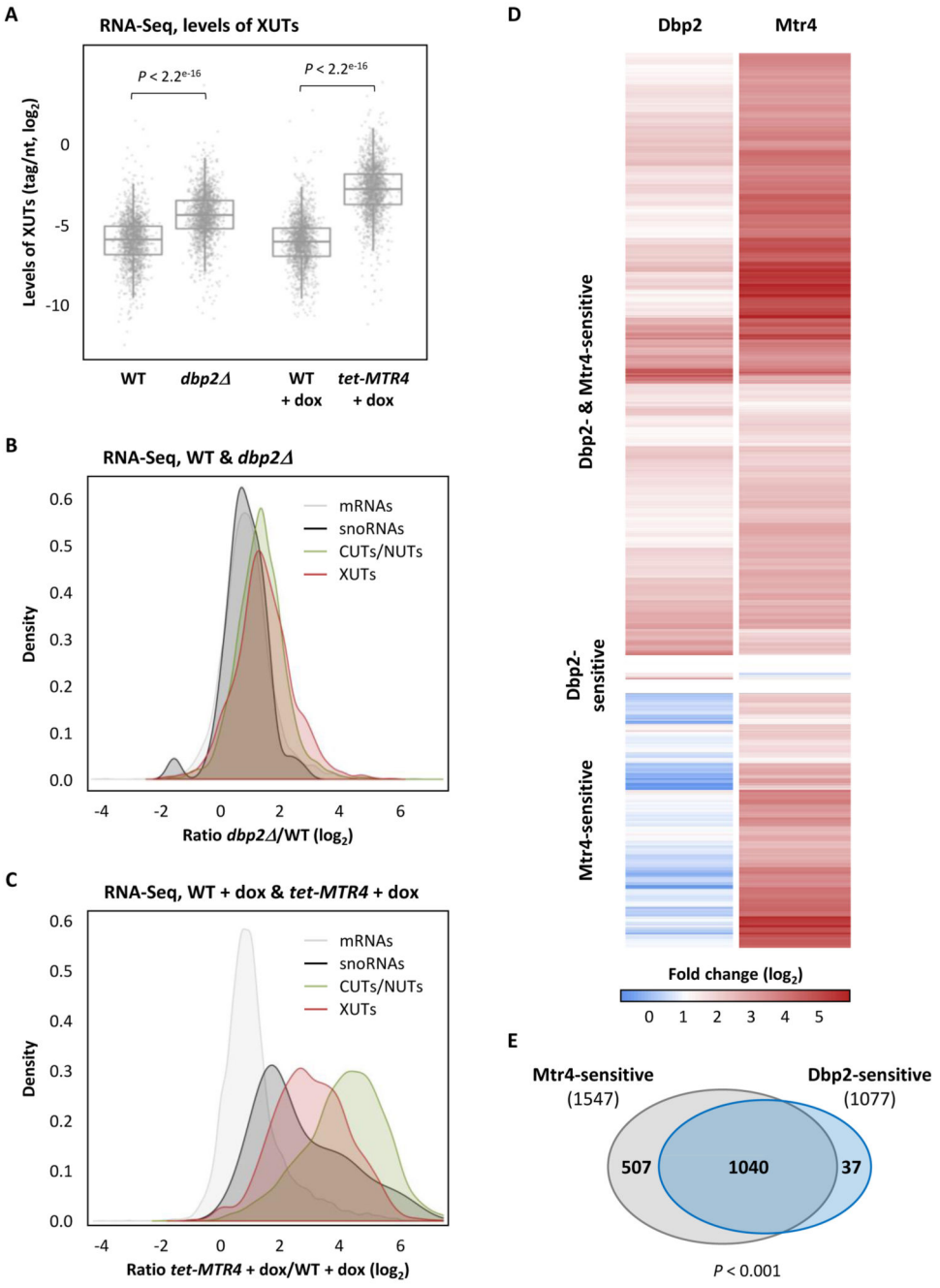


**Figure 1.**

Identification of Dbp2-and Mtr4-sensitive XUTs. **(A)** Total RNA-Seq was performed using total RNA extracted from two biological replicates of exponentially growing YAM1 (WT) and YAM2627 (*dbp2Δ*) cells, as well as YAM115 (WT) and YAM997 (*tetOFF::MTR4*) cells grown in the same conditions and then treated for 6 h with doxycycline (dox, 10 µg/mL final concentration). The data are presented as densities (tag/nt, $\log_2$ scale) for XUTs. The indicated *p*-values were obtained upon two-sided Wilcoxon rank-sum test (adjusted for multiple testing with the Benjamini–Hochberg procedure). **(B)** Density-plot of the

expression fold-change (ratio of tag densities, $\log_2$ scale) for mRNAs (grey), snoRNAs (black), CUTs/NUTs (green) and XUTs (red). **(C)** Same as above for *tet-MTR4* + dox/WT + dox. **(D)** Heatmap of the expression fold-change ($\log_2$) for the Dbp2-and/or Mtr4-sensitive XUTs in cells lacking Dbp2 (*dbp2Δ*) or depleted for Mtr4 (*tet-MTR4* + dox), relative to the isogenic WT control. **(E)** Venn diagram showing the number of Dbp2-sensitive (1077) and Mtr4-sensitive XUTs (1547). The *p*-value obtained upon Chi-square test of independence is indicated. See also Supplementary Table S1.



Europe PMC Funders Author Manuscripts

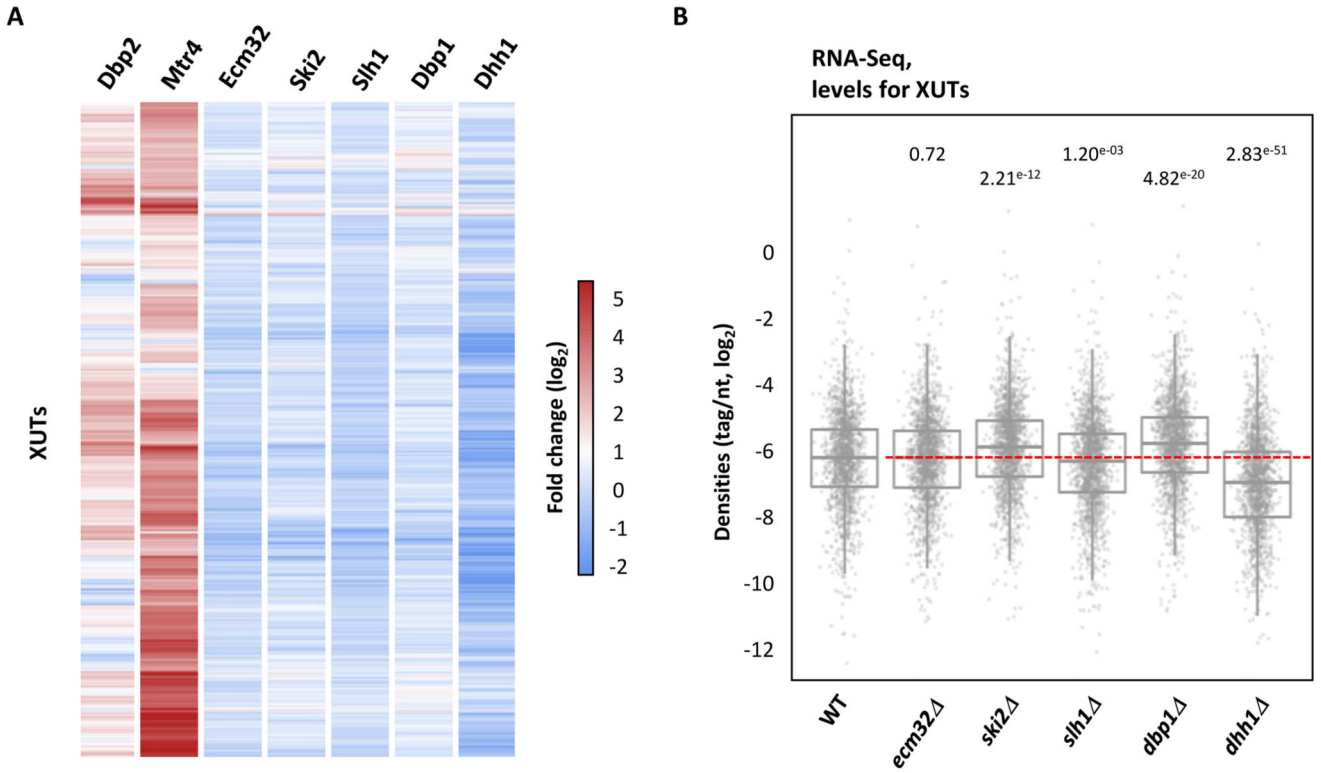


**Figure 2.**

XUTs do not globally accumulate upon inactivation of the Ecm32, Ski2, Slh1, Dbp1 and Dhh1 RNA helicases. **(A)** Total RNA-Seq was performed using total RNA extracted from two biological replicates of exponentially growing YAM1 (WT), YAM2834 (*ecm32Δ*), YAM2628 (*ski2Δ*), YAM2835 (*slh1Δ*), YAM2630 (*dbp1Δ*) and YAM2632 (*dhh1Δ*). Data are presented as a heatmap of XUTs expression fold-change (ratio of tag densities, $\log_2$ scale) for each mutant relative to the WT control. The fold-change for XUTs in Dbp2-lacking and Mtr4-depleted cells is shown for comparison. **(B)** Box-plot showing densities (tag/nt, $\log_2$ scale) for XUTs in WT, *ecm32Δ*, *ski2Δ*, *slh1Δ*, *dbp1Δ* and *dhh1Δ* cells. The indicated *p*-values were obtained upon two-sided Wilcoxon rank-sum test (adjusted for multiple testing with the Benjamini–Hochberg procedure).

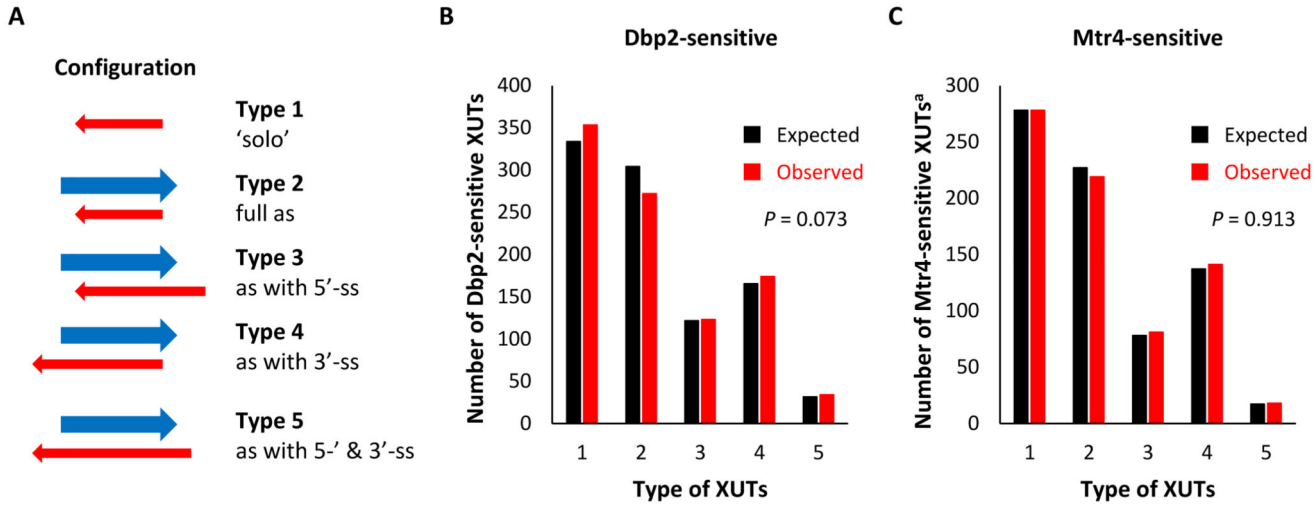


**Figure 3.**

Dbp2 and Mtr4 target XUTs independently of their configuration to protein-coding genes. **(A)** Schematic representation of the five types of XUTs, defined according to their configuration relative to sense mRNAs. The red and blue arrows represent the XUT and the paired-sense mRNA, respectively. **(B)** Bar-plot showing the number of XUTs of each type among the set of Dbp2-sensitive XUTs. The black and red bars indicate the numbers expected by chance and observed experimentally by RNA-Seq, respectively. **(C)** Same as above for the Mtr4-sensitive XUTs[a] subset.




Europe PMC Funders Author Manuscripts

Europe PMC Funders Author Manuscripts

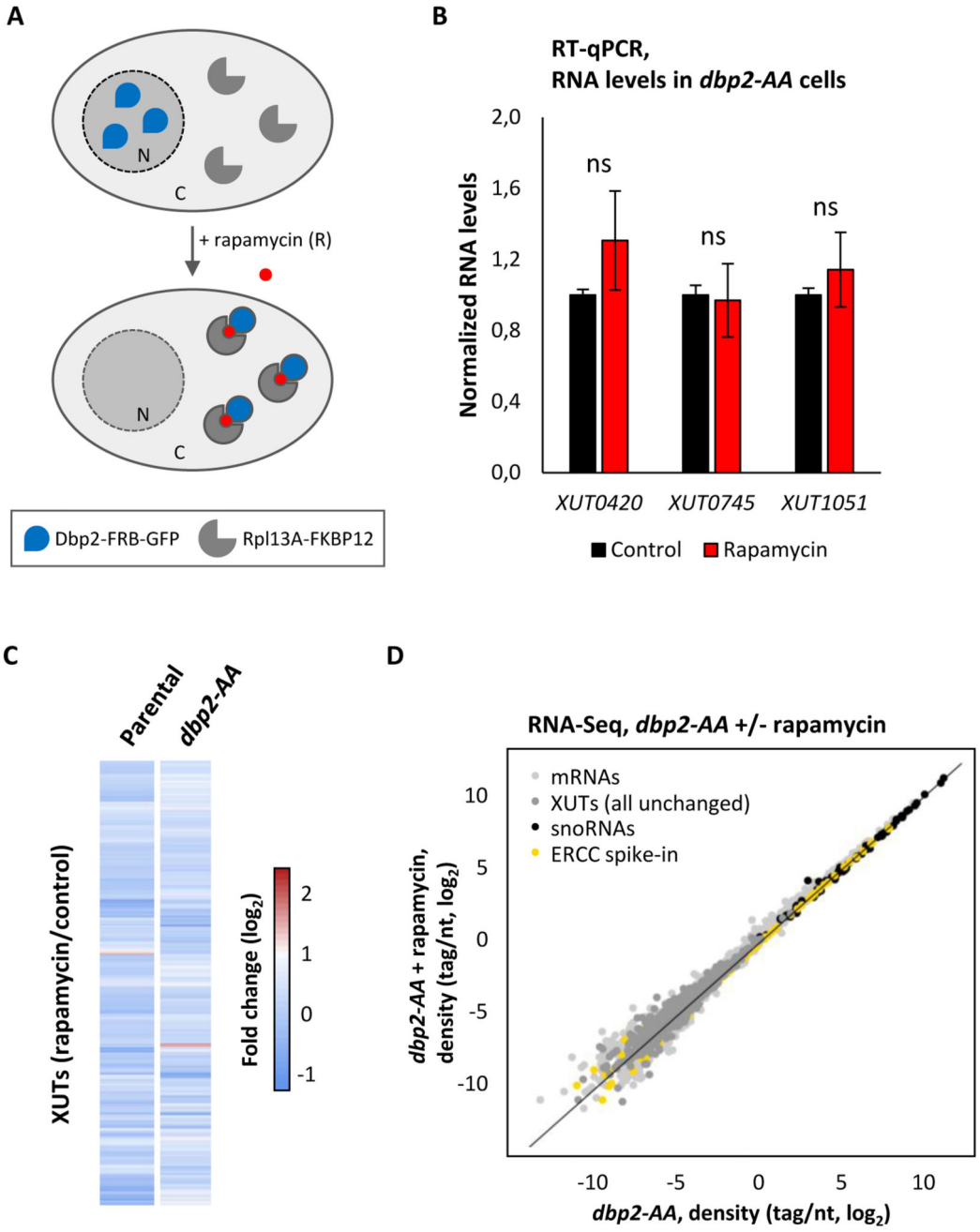


**Figure 4.**

XUTs are insensitive to Dbp2 nuclear depletion. **(A)** Schematic representation of the Dbp2 anchor-away experiment. **(B)** YAM2673 (*dbp2-AA*) cells were grown to mid-log phase, at 30°C, in YPD medium and then treated for 60 min with 1 µg/mL (final concentration) of rapamycin. After total RNA extraction, the levels of *XUT0420*, *XUT0745* and *XUT1051* were assessed by strand-specific RT-qPCR, and then normalized on the *PMA1* mRNA (unaffected housekeeping gene). The normalized level of each XUT in the untreated condition was set to 1. Mean and SD values were calculated from three independent

biological replicates. ns, not significant upon *t*-test. **(C)** Total RNA-Seq was performed using total RNA extracted from YAM2672 (parental) and YAM2673 (*dbp2-AA*) cells grown as above. The data are presented as a heatmap of the expression fold-change ($log_2$) for XUTs in WT and *dbp2-AA* cells following rapamycin treatment relative to the untreated control condition. **(D)** RNA-Seq signals in YAM2673 (*dbp2-AA*) cells grown as above and treated or not with rapamycin. The data are presented as densities (tag/nt, $log_2$ scale) for mRNAs (light grey), XUTs (dark grey) and snoRNAs (black) upon normalization on the ERCC spike-in (yellow).